Supplementary Information

Method

Synthesis of $Li_4Mn_5O_{12}$-like. We used a low-temperature solid-sate synthesis method to prepare spinel $Li_4Mn_5O_{12}$-like samples. First, $MnCO_3$ (Aladdin, 99.95%) was mixed with $LiOH·H_2O$ (Adamas, 99%). The molar ratio of $MnCO_3$: $LiOH·H_2O$ was 5:4. After ground for 1 h, the obtained mixture was sintered at 400°C for 12 h under air atmosphere to get the final material.

Material characterizations. X-ray diffraction was performed on Rigaku Ultima Ⅳ. It was operated in the 2θ value range of 10° to 80° with a 2°/min scanning rate. The morphology of the $Li_4Mn_5O_{12}$-like sample was identified by Quanta 200 filed emission scanning electron microscope (FESEM). The HRTEM images were taken on a transmission electron microscope JEM-2100F with accelerating voltage of 200 kV. X-ray photoelectron spectroscopy (XPS) measurement was carried out by use of ESCALAB 250Xi.

Electrochemical tests. CR2025-type coin cells, assembled in a glove box filled with dry argon gas, were used for electrochemical tests. A coin cell consisted of a positive electrode, an anode, ceramic membrane and organic electrolyte. To fabricate the positive electrode, active materials and carbon black (electron conduction) were ground with the weight ratio of 90:5. Then the as-prepared materials were mixed with polyvinylidene fluoride (PVDF) binder (95:5, weight ratio) in appropriate amount of N-methylpyrrolidone (NMP), using magnetic stirring to mix fully. The obtained slurry

was cast onto an aluminum foil current collector. Then, it was dried at 80°C overnight in vacuum. The organic electrolyte was 1mol/L $LiPF_6$ in a mixture of equal volumes of ethylene carbonate (EC) and dimethyl carbonate (DMC). For half cells and full cells, the anodes were lithium metal and lithium-tin alloy respectively. The electrochemical tests were carried out on a battery test system (Neware). Electrochemical impedance spectroscope (EIS) data was performed on a CHI600A Electrochemical workstation (Chinster, Shanghai, China), with 5mV ac excitation over a frequency range of 1 mHz to 100 kHz. Cyclic voltammogram (CV) test was performed at a scan rate of 0.1 mV s^{-1} among voltage range of 1.8 V to 4.7 V (*vs.* Li^+/Li) by a CHI600A Electrochemical workstation (Chinster, Shanghai, China).

Result and discussion

The low-temperature solid-state synthesis process is illustrated in Fig. S1. $Li_4Mn_5O_{12}$-like cathode is prepared through a solid-state process, which is very simple and scalable.

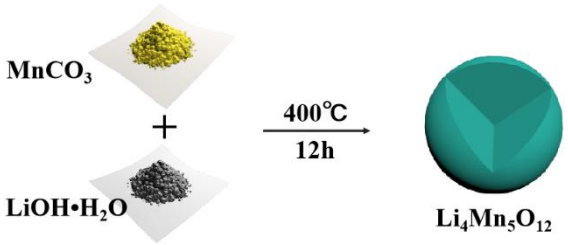

Fig. S1. The synthesis schematic diagram of $Li_4Mn_5O_{12}$-like nanoparticulates.

The microstructure and morphology of $Li_4Mn_5O_{12}$-like powders are also observed through field emission scanning electron microscopy (FE-SEM), as shown in Fig. S2a and S2b. Secondary microparticles with a diameter of around 5 μm could be seen (Fig. S2a) and closer observation in Fig. S2b reveals that the secondary particles are self-assembled by primary nanoparticles.

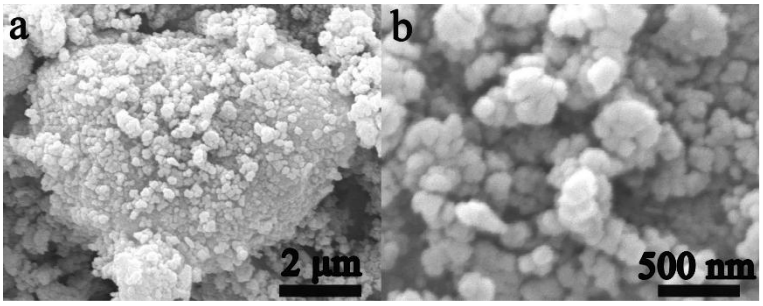

Fig. S2. (a) and (b) SEM images of $Li_4Mn_5O_{12}$-like nanoparticulates, which self-assemble into secondary particles.

From the high-resolution transmission electron microscopy (HRTEM) image in Fig. S3, interplanar spacing of 0.471 nm and 0.239 nm, which are corresponded to the [111] and [222] planes of spinel $Li_4Mn_5O_{12}$ structure, respectively, are identified. It is generally believed that such nano-sized crystallinity could effectively accommodate the strain of Jahn-Teller though slippage at the domain wall boundaries, and thus is beneficial to the stability of cathode material.[1-3]

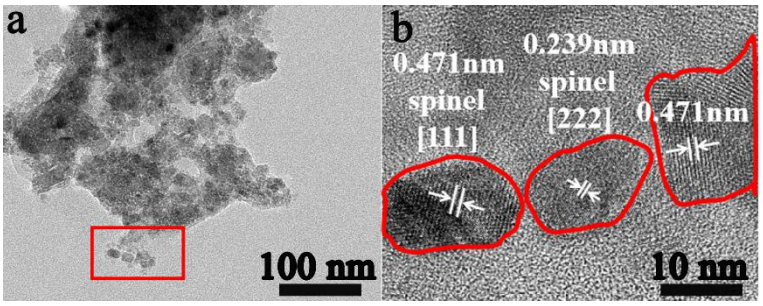

Fig. S3. (a)TEM and (b)HRTEM images of $Li_4Mn_5O_{12}$-like nanoparticulates, which self-assemble into secondary particles.

The CV curve (in Fig. S4) also indicates that there are two lithium storage processes, corresponding to two redox peaks at ~ 2.8 V and ~ 4 V respectively during discharge process of $Li_4Mn_5O_{12}$-like cathode.

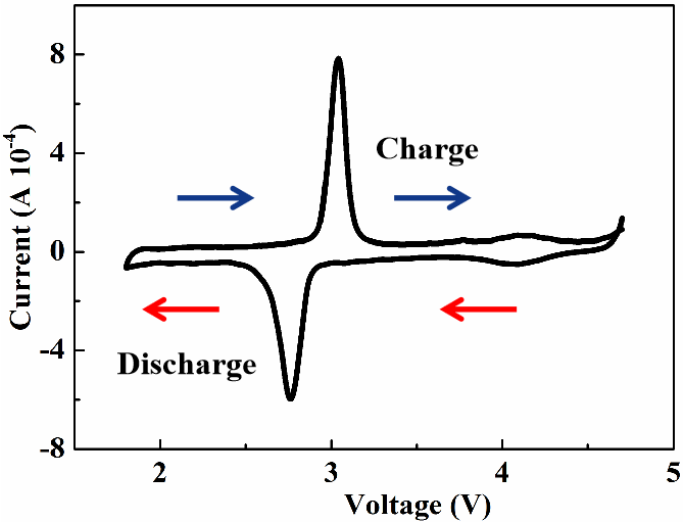

Fig. S4. CV curve of $Li_4Mn_5O_{12}$-like.

Thanks to the cubic structure of spinel $Li_4Mn_5O_{12}$ with three-dimensional Li diffusion channels, this cathode shows good rate performance with small impedance during cycling, as revealed in Fig. S5.

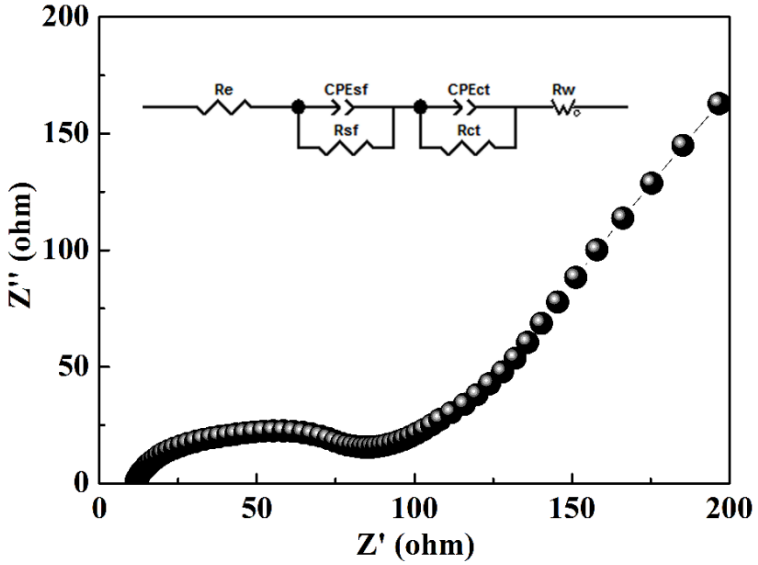

Fig. S5. Equivalent circuit model and Nyquist plots of $Li_4Mn_5O_{12}$-like.

The full cells were assembled by pairing the $Li_4Mn_5O_{12}$-like cathode against Li_xSn anode[4] and tested at a current density of 100 mA g^{-1} between 1.0 and 4.1 V at room temperature. As shown in Fig. S6a and S6b, the initial discharge capacity reaches 213 mA h g^{-1}. After 45 cycles, the capacity stabilizes at 204 mA h g^{-1} with hardly any capacity attenuation.

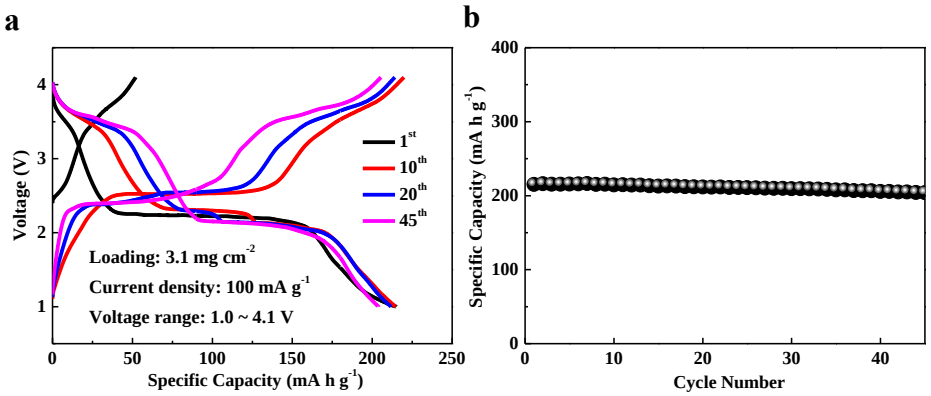

Fig. S6. (a) Charge/discharge curves of $Li_4Mn_5O_{12}$-like full cells from the 1st cycle to the 45th cycle at a current density of 100 mA g^{-1} among 1.0 ~ 4.1 V at room temperature, (b)cycling performance of $Li_4Mn_5O_{12}$-like full cells.

In Fig. S7, cation- and anion-redox capacities evolving over cycles were examined individually, where an anion-redox capacity increment during the first 30 cycles was observed, probably due to an activation process of oxygen. In the subsequent cycles, a slow decline that might be related to oxygen release could be found. Meanwhile, cation-redox capacity deteriorates gradually with prolonged cycling, which is possibly

attributed to the dissolution of manganese and the damage of structure.

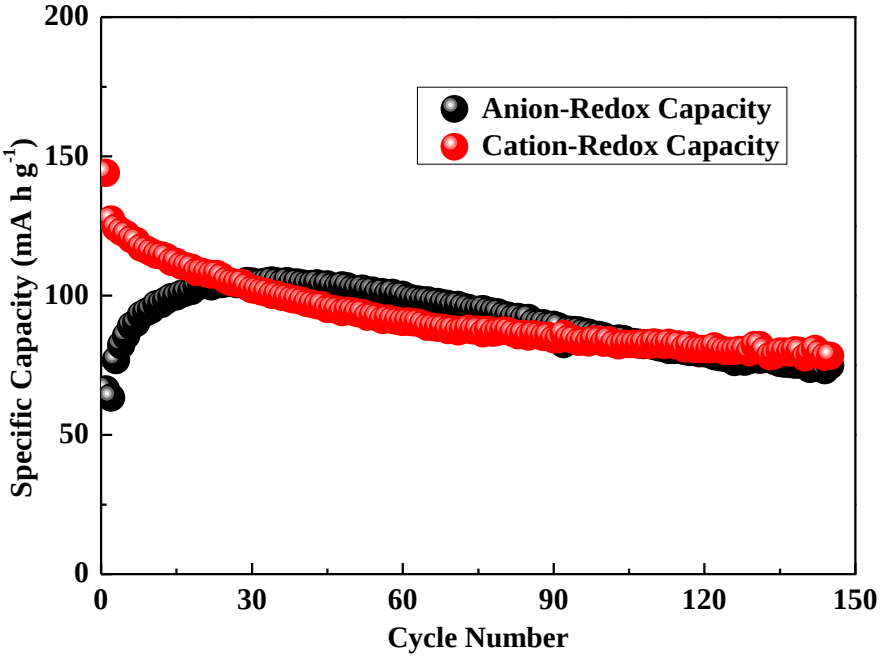

Fig. S7. The cation- and anion-redox capacities evolving over cycles of $Li_4Mn_5O_{12}$-like cathode.

In Fig. S8, the derivative capacity vs. voltage of $Li_4Mn_5O_{12}$-like cathode is calculated by the data of the 20th cycle (presented in Fig. 3b). The main redox peaks are at ~ 2.8 V and ~ 4 V, which correspond to two reactions above mentioned.

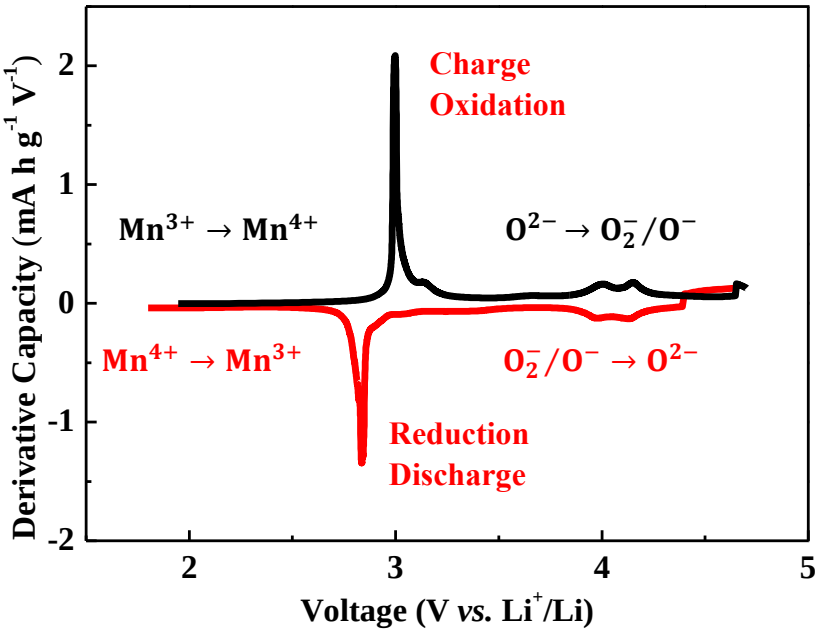

Fig. S8. Derivative capacity vs. voltage curve of $Li_4Mn_5O_{12}$ system during the 20th cycle.

$Li_4Mn_5O_{12}$-like cathode could have excellent cost-performance ratio. Compared

with the benchmark cathode materials, such as $LiFePO_4$, $LiCoO_2$, $LiNiO_2$ and $Li(Ni_xCo_yMn_{1-x-y})O_2$, our $Li_4Mn_5O_{12}$-like cathode can deliver a high capacity of 213 mA h g^{-1}, which behaves better than $LiFePO_4$ (162 mA h g^{-1}), $LiCoO_2$ (140 mA h g^{-1}), and $LiNi_{1/3}Co_{1/3}Mn_{1/3}O_2$ (200 mA h g^{-1}).[5-7] The cost of our cathode material is less than \$ 5.72 kg^{-1}, which is one fifth of the cost of $LiCoO_2$ (\$ 26.24 kg^{-1}), a quarter of the cost of $LiNi_{1/3}Co_{1/3}Mn_{1/3}O_2$ (\$ 20.99 kg^{-1}) and about one third of the cost of $LiFePO_4$ (\$ 12.72 kg^{-1}), as exhibited in Fig. S9.

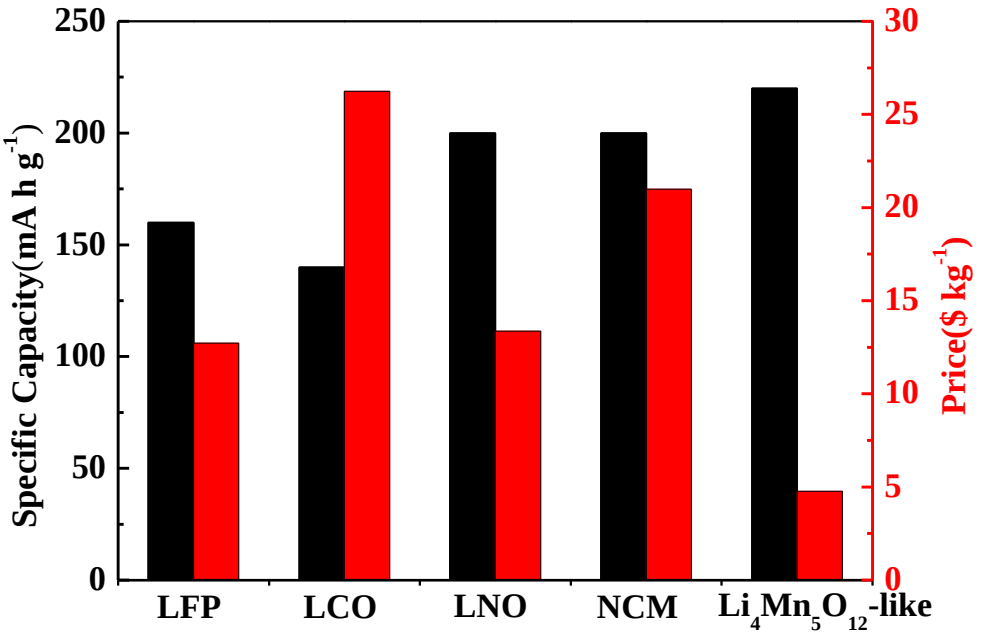

Fig. S9. Specific capacities and price of $LiFePO_4$ (LFP), $LiCoO_2$ (LCO), $LiNiO_2$ (LNO), $Li(Ni_xCo_yMn_{1-x-y})O_2$ (NCM) and $Li_4Mn_5O_{12}$-like.

The tap density of well-prepared $Li_4Mn_5O_{12}$-like cathode is about 3 g cm^{-3}. Therefore, the volumetric energy density of $Li_4Mn_5O_{12}$-like cathode is estimated to be as high as 2060 W h L^{-1}. This value is quite competitive, compared to LFP and even NCM, but we believe it could be further optimized because, at the present stage, the primary particles is very small. And the volumetric energy density remains at 1450 W h L^{-1} after 145 cycles.

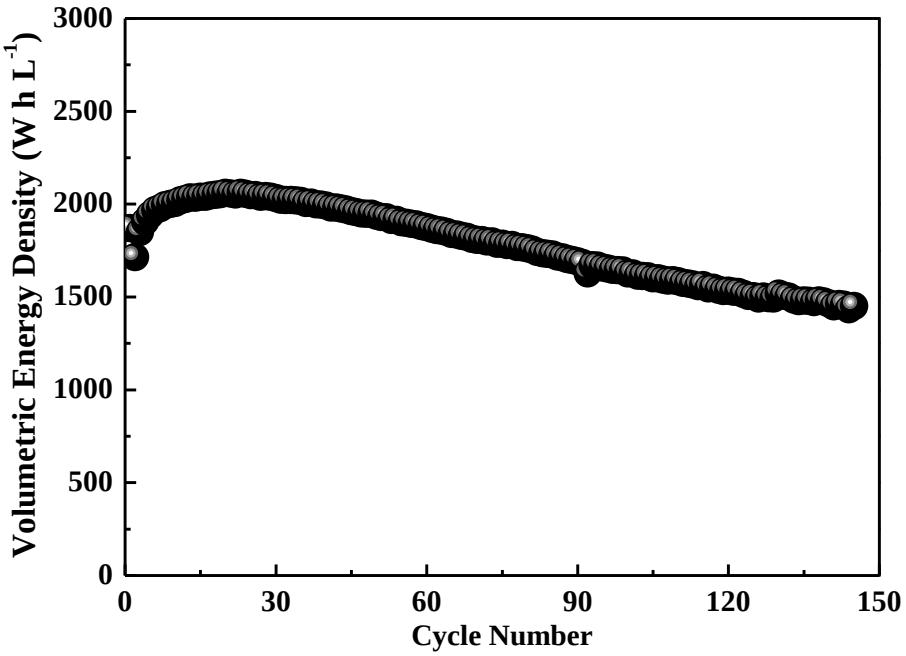

Fig. S10. Volumetric energy density of $Li_4Mn_5O_{12}$-like half cells from the 1st cycle to the 145th cycle at a current density of 100 mA g^{-1} within a voltage window of 1.8 ~ 4.7 V *versus* Li^+/Li at room temperature.

Table S1 Linear fitting data of Williamson-Hall (W-H) plots (in Fig. 1c).

Equation	y = a + b*x		
Weight	No Weighting		
Residual Sum of Squares	1.68255E-5		
Pearson's r	-0.81481		
Adj. R-Square	0.6159		
		Value	Standard Error
B	Intercept	0.01449	0.00203
B	Slope	-0.00246	6.62668E-4

References

1. H. Wang, Y. I. Jang and Y. M. Chiang, *Electrochemical and Solid-State Letters*, 1999, **2**, 490-493.
2. Y. I. Jang, B. Huang, Y. M. Chiang and D. R. Sadoway, *Electrochemical and Solid-State Letters*, 1998, **1**, 13-16.

3. Y. Shao‐Horn, S. A. Hackney, A. R. Armstrong, P. G. Bruce, R. Gitzendanner, C. S. Johnson and M. M. Thackeray, *Journal of the Electrochemical Society*, 1999, **146**, 2404-2412.
4. H. Xu, S. Li, C. Zhang, X. L. Chen, W. J. Liu, Y. H. Zheng, Y. Xie, Y. H. Huang and J. Li, Energy Environ. Sci., 2019, 10.1039/C9EE01404G.
5. A. Yamada, S.-C. Chung and K. Hinokuma, *Journal of the Electrochemical Society*, 2001, **148**, A224-A229.
6. T. Ohzuku, A. Ueda, M. Nagayama, Y. Iwakoshi and H. Komori, *Electrochimica Acta*, 1993, **38**, 1159-1167.
7. N. Yabuuchi and T. Ohzuku, *Journal of Power Sources*, 2003, **119**, 171-174.